A High-Gain Array Antenna Design for 6G Terahertz Wireless Systems

Dasari Nataraj
Department of ECE, Swarnandhra College of Engineering and Technology, Narsapur, India
dasari.nataraj@gmail.com

Karedla Chitambara Rao
Department of ECE, Aditya Institute of Technology and Management, Tekkali, India
rao.chiddubabu@gmail.com (corresponding author)

K. S. Chakradhar
Department of ECE, Mohan Babu University, Tirupati, India
chakradharec@gmail.com

B. Sudhir
Department of ECE, International School of Technology and Sciences for Women, East Gonagudem, Rajanagaram, Rajahmundry, India
bsudhir539@gmail.com

G. Vinutna Ujwala
Department of ECE, St. Martin's Engineering College, Secunderabad, India
ujwala459@gmail.com

M. Lakshmunaidu
Department of ECE, Koneru Lakshmaiah Education Foundation, Vaddeswaram, India
laxman.naidu@gmail.com

Pedada Kameswara Rao
Department of ECE, Aditya Institute of Technology and Management, Tekkali, India
kameshpedada@gmail.com

Received: 13 April 2025 | Revised: 28 May 2025 and 10 June 2025 | Accepted: 14 June 2025

 DOI: https://doi.org/10.48084/etasr.11467

ABSTRACT

The increasing demand for ultra-high-speed wireless communication and large data rates is driving the development of Sixth Generation (6G) networks, which are expected to have become commercially available around 2030. To support emerging applications, such as the Internet of Nano-Things (IoNT), high-speed on-chip communication, real-time health monitoring, and satellite connectivity, 6G systems will rely on the Terahertz (THz) frequency spectrum (0.1–10 THz). However, high propagation losses at these frequencies necessitate the use of high-gain antennas. One promising solution is the implementation of multi-element antenna arrays. This study presents the design of a compact 1×4 linear array antenna based on a triangular slot technique, aimed at improving performance in the THz band for 6G applications. The antenna is fabricated on a 10 µm-thick quartz substrate with a dielectric constant of 3.8 and a loss tangent of 0.0001. Gold layers form the radiating and ground surfaces, and a parallel feedline ensures a uniform power distribution. The simulations performed in CST software demonstrated favorable results, with a maximum gain of 11 dBi, a wide operating bandwidth of 1 THz (0.6–1.6 THz), and a return loss of −28 dB. The design also exhibits reduced mutual coupling (−18 dB), contributing to enhanced array performance. These results highlight the antenna's potential for efficient integration into future high frequency 6G communication systems.

Keywords-rectangular microstrip patch antenna; terahertz frequency band; triangular slot technique; parallel feeding; 6G wireless communication

I. INTRODUCTION

As industries, healthcare, transportation, space, and maritime systems become increasingly automated, the modern society is advancing toward full-scale automation. In this environment, billions of sensors will need to be integrated into a wide variety of systems. High data rates and reliable connectivity will, therefore, be essential for sophisticated wireless communication. The 6G communication system is expected to meet these requirements, offering ultra-high data rates, low latency, wide bandwidth, and fast data transmission speeds. To improve the wireless performance and support the growing traffic demands, 6G is anticipated to play a vital role.

For 6G systems operating in the THz frequency range, a multi-slotted elliptical patch antenna has been proposed with several optimizations. This antenna demonstrates notable performance, achieving a gain of 7.769 dB, an operational bandwidth of 1.25 THz, and a return loss of −27.08 dB. It is fabricated on a Rogers 5880 substrate [1]. The co-axial feeding technique has also been used to develop a compact rectangular dual patch antenna for satellite communication applications [2].

However, designing effective THz-band antennas remains a significant challenge, particularly in terms of efficiency, gain, and bandwidth critical factors for high-frequency applications. As a result, the development of high-performance THz antennas is crucial for realizing the full potential of 6G networks [3]. In [4], a dual-band reconfigurable graphene-based antenna achieved a gain of 6.793 dBi, a bandwidth of 26.7 GHz, and a return loss of −64.16 dB. Defective Ground Structures (DGS) and Photonic Band Gaps (PBG) were employed in [5] to enhance performance, resulting in a bandwidth of 50 GHz, a gain of 4.01 dBi, and a return loss of −21.67 dB. However, this method did not effectively address the size and bandwidth limitations.

Another study demonstrated a compact graphene-based patch antenna operating in the THz band, which offered a return loss of −57.54 dB and a bandwidth of 199.6 GHz, though its gain was limited to 2.76 dB [6]. An asymmetric coplanar waveguide-fed patch antenna was developed with a compact design, a bandwidth of 38 GHz, a gain of 5 dBi, and a return loss of −28 dB [7]. A circular ring enclosed by a square-shaped ring has also been proposed as the radiating element. This antenna, designed with a partial ground plane, achieved wideband performance with a bandwidth of 0.415 THz. To increase the gain, two L-shaped stubs were introduced, resulting in a return loss of −24.5 dB and a peak gain of 5.87 dBi [8].

Further improvements in impedance matching, radiation efficiency, and return loss have been achieved through slot-loading techniques. One such design attained a bandwidth of 92 GHz, a gain of 6.14 dBi, and a return loss of −16.86 dB [9].

Beyond communication, the THz band also supports applications in industrial quality control and security scanning through THz imaging and non-invasive sensing [10]. However, the THz transmission still faces several challenges, including severe air attenuation and limited short-range connectivity [11].The shape of the antenna's patch plays a critical role in determining its overall performance. Previous studies have examined a variety of patch geometries, such as rectangular and circular [12]. In [5, 13], PBG structures were used to improve the antenna behavior. With return losses of −64.16 dB and −26.27 dB, bandwidths of 24 GHz and 20 GHz, and gains of 6.79 dBi and 6.32 dBi, respectively, the curvature radius of the PBG influenced both the gain and directivity [14].

Array-based designs have also been explored. For example, by suppressing surface waves in a uniform substrate, their performance was analyzed within the 0.69–0.72 THz range, achieving a gain of 9.75 dBi, a bandwidth of 0.03 THz, and a return loss of −67.2 dB. Reconfigurable fractal antennas incorporating electro-optic substrate materials have also been introduced [15], demonstrating a gain of 4.92 dBi, a bandwidth of 36 GHz, and a return loss of −14.5 dB.

Metamaterial and surface-integrated waveguide techniques were employed in [16] to enhance performance, leading to a gain of 1.8 dBi, a bandwidth of 22 GHz, and a return loss of −34 dB. Additionally, a high-gain THz array antenna based on the PCB technology and the SIW structure was constructed, offering a peak gain of 13.14 dBi at 0.61 THz.

The high-gain operation in THz frequencies is critical for improving the signal quality and reducing the noise, which is essential for long-range communication. In radar and point-to-point systems, such antennas focus energy into narrow beams, enabling effective use of the THz technology in communication, imaging, and sensing applications [11].

II. ANTENNA DESIGN AND PERFORMANCE RESULTS

The proposed 1×4 linear array antenna is designed in four steps. Each stage involves three different materials: the substrate, the patch, and the ground plane, with the dimensions of each material clearly specified. The antenna is built on a quartz substrate with a thickness of 10 µm, a loss tangent of 0.0001, and a dielectric constant of 3.8. The upper and lower surfaces are gold-plated, serving as the radiating patch and the ground plane, respectively. A parallel feedline structure is employed as the feeding mechanism. Quartz was selected as the substrate material due to its high mechanical strength and favorable dielectric properties.

To achieve a compact size and high gain, triangular slots are introduced into the rectangular microstrip patch. These slots extend the effective current path without increasing the overall physical dimensions, thereby enhancing the performance without compromising the design compactness.

A. Step 1: Design of a Single Inset-Fed Microstrip Patch Antenna

In the first step, a single inset-fed rectangular microstrip patch antenna is designed based on [8]:

$$w = \frac{c}{2f_r}\sqrt{\frac{2}{\varepsilon_r+1}} \quad (1)$$

where w corresponds to the width of the microstrip patch.

$$\varepsilon_{reff} = \frac{\varepsilon_r+1}{2} + \frac{\varepsilon_r-1}{2}\left(1+12\frac{h}{w}\right)^{\frac{-1}{2}} \quad (2)$$

where ε_{reff} represents the effective dielectric constant of the microstrip patch.

$$L_{eff} = \frac{c}{2f_r\sqrt{\varepsilon_{reff}}} \quad (3)$$

where L_{eff} represents the effective length of the patch.

$$\Delta L = 0.421h\frac{(\varepsilon_r+0.3)(\frac{w}{h}+0.264)}{(\varepsilon_r-0.258)(\frac{w}{h}+0.8)} \quad (4)$$

where ΔL represents the additional length of the patch.

$$L = L_{eff} - 2\Delta L \quad (5)$$

where L denotes the length of the microstrip patch.

$$L_g = 6h + L \quad (6)$$

where L_g stands for the ground's length.

$$w_g = 6h + w \quad (7)$$

where w_g stands for the ground's width.

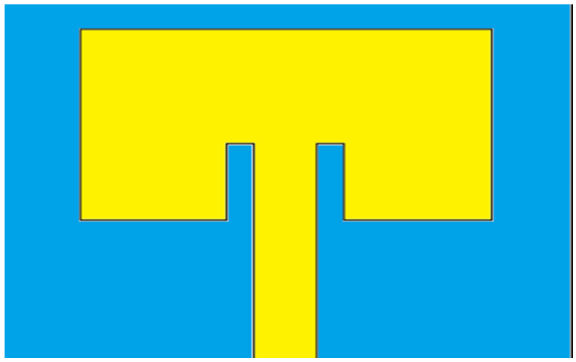

Fig. 1. Rectangular microstrip patch antenna.

TABLE I. DESIGN PARAMETERS

Design parameter	Values in step 1 (μm)	Values in step 2 (μm)
Patch width	121.03	100.5
Patch length	96.05	92.66
Width of ground and substrate	181.03	179.54
Length of ground and substrate	156.05	150.50
Width of the feed	23.53	23.53
Inset feed length	38.64	38.64
Notch gap	10	10
Total length of the feed	108.41	108.41
Gap between notch and edge	28.49	28.49

The rectangular microstrip patch antenna, designed to operate at 0.8 THz, is shown in Figure 1. As presented in Table I, the antenna exhibits relatively large dimensions in terms of length and width. This results in an overall increase in its physical size, which may be undesirable in compact system designs. Therefore, the size reduction is an important design consideration. According to the return loss *(S_{11})* curve displayed in Figure 2, a significant dip is observed at 0.8 THz, indicating a notable decrease in the return loss.

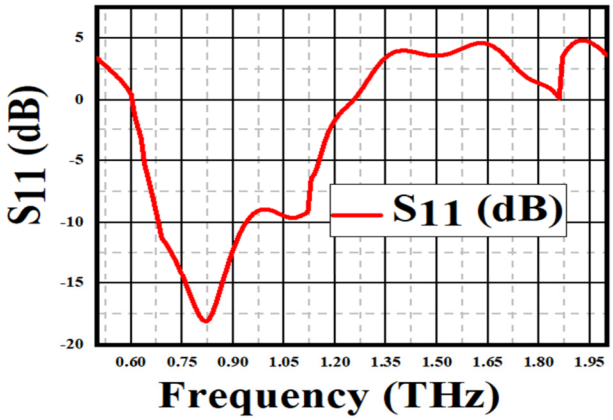

Fig. 2. Return loss *(S_{11})* of the rectangular microstrip patch antenna.

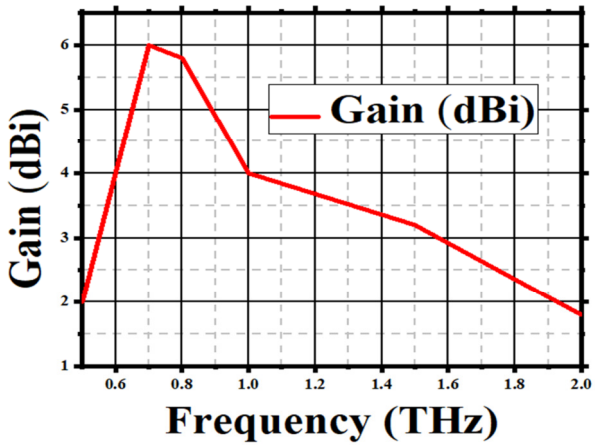

Fig. 3. Gain of the rectangular microstrip patch antenna.

Figure 3 shows that an antenna performs best at a frequency of about 0.8 THz, with a peak gain of about 5.8dBi. After that, the gain progressively drops, reaching about 2 2dBi at 2.0 THz.

B. Step 2: Design of Single Inset-Fed Microstrip Patch Antenna With Triangular Slots Technique

Step 1 results in the maximum width and length values for the antenna. To reduce these dimensions while preserving key performance parameters, such as gain and return loss *(S_{11})*, the triangular slot technique is applied to the rectangular microstrip patch at a frequency of 0.8 THz. This method enables a size reduction without compromising the antenna's electromagnetic performance.

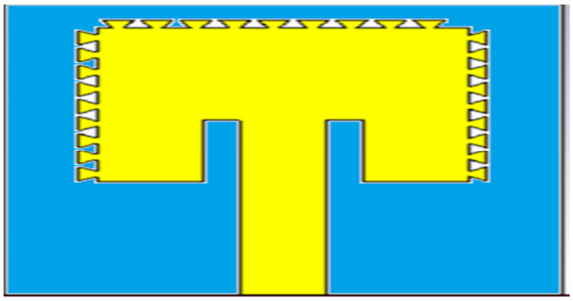

Fig. 4. Rectangular microstrip patch antenna with triangular slots.

A triangular-slotted, rectangular microstrip patch antenna is depicted in Figure 4. It is made using triangular slots as a model. The antenna's size was decreased, and the electrical path length was extended by adding triangular slots to the rectangular microstrip patch. The antenna also showed better impedance matching, a wider bandwidth, gain, and a lower return loss after the addition of triangular slots. By reducing the surface wave losses, the slots also improved the radiation efficiency. Table I lists the design parameters following the application of the triangular slot approach.

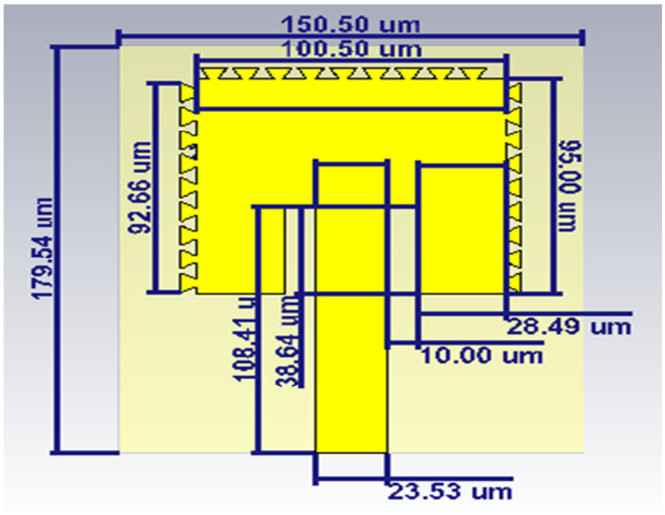

Fig. 5. Dimensional parameters of the rectangular MPA with triangular slots.

Figure 5 portrays the dimensional values of the rectangular microstrip patch antenna with the triangular slot technique.

According to Table I, the triangular slot approach in Step 2 resulted in a modest reduction in the patch dimensions and overall substrate size when compared to the design parameters from Step 1. The Step 1 design does not employ any technique. Furthermore, the feed line shape and dimensions associated with the notch do not change. The graph in Figure 6 demonstrates a notable decrease in the return loss at 0.8 THz, with a return loss (S_{11}) falling below -18 dB (-21 dB), indicating good impedance matching at this frequency.

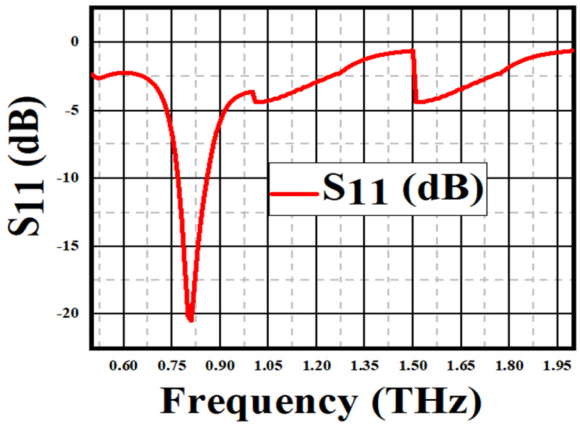

Fig. 6. Return loss (S_{11}) of the rectangular microstrip patch antenna with triangular slots.

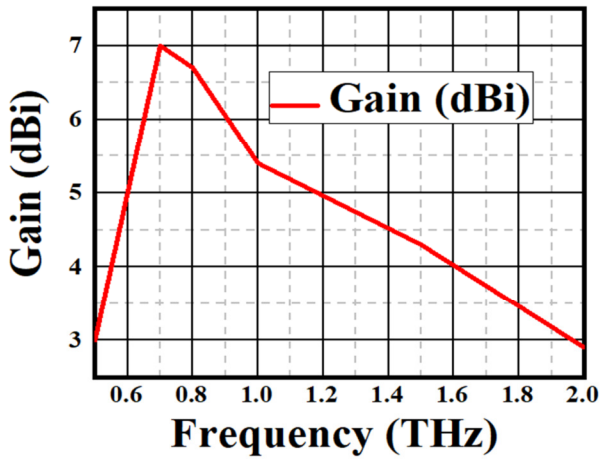

Fig. 7. Gain of the rectangular patch antenna with triangular slots.

The antenna exhibits an optimal radiation performance at 0.8 THz, as indicated by the graph in Figure 7, which shows a peak gain of 7dBi.

C. Step 3: Coupling Coefficient Between Two Patch Antennas

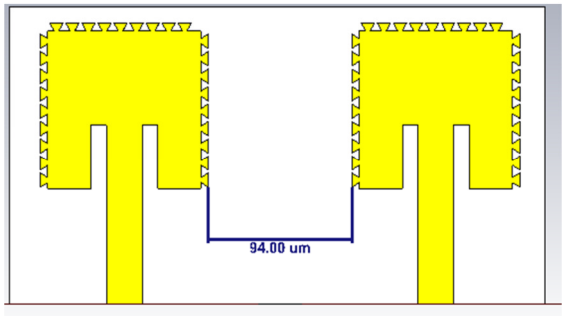

Fig. 8. Geometry of the 1×2 linear array antenna.

The 1×2 linear array antenna is illustrated in Figure 8. To enhance the gain for wireless communication applications, two microstrip patch antenna elements are arranged in a 1×2

configuration, forming a linear antenna array. In this stage, the mutual coupling coefficient between the two patches is evaluated by positioning them at an edge-to-edge separation distance of 94 µm.

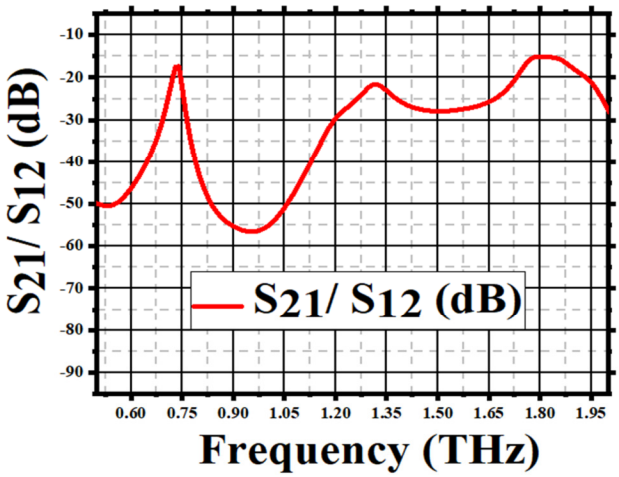

Fig. 9. Return loss (S_{11}) of the 1×2 linear array antenna.

The transmission coefficients, S_{21} and S_{12}, are shown in Figure 9. The lowest losses occur at 0.8 THz, indicating a strong signal transmission and efficient coupling between the antenna elements at this frequency. At other frequencies, the transmission coefficients drop significantly, suggesting an increased isolation and reduced mutual coupling. The peaks in the S_{21}/S_{12} response correspond to frequencies where the energy transfer between the elements is more efficient, reflecting higher levels of coupling.

D. Step 4: Design of 1x4 Linear Array Antenna

The 1×4 linear array antenna is illustrated in Figure 10. To increase the gain, four microstrip patch antenna elements are arranged in a 1×4 configuration. A parallel line feeding technique is employed to ensure that all four patches receive equal power. The physical dimensions of the 1×4 array are shown in Figure. 11.

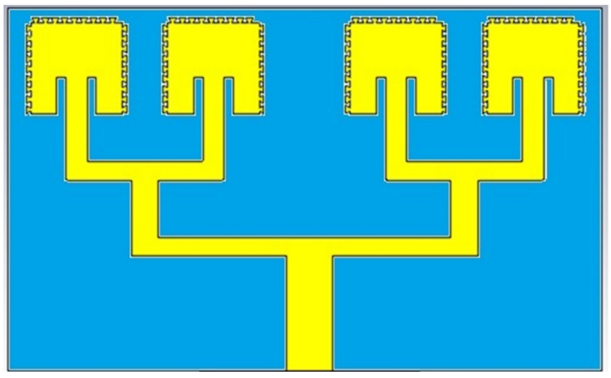

Fig. 10. 1×4 linear array antenna.

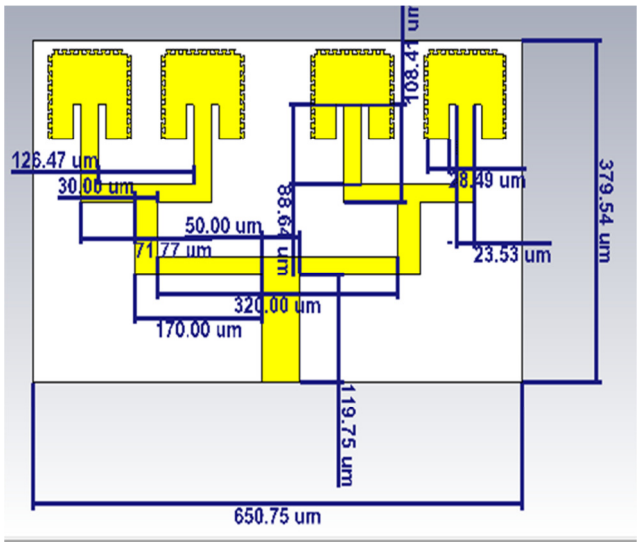

Fig. 11. Dimensional parameters of the 1×4 array antenna.

TABLE II. DESIGN DIMENSIONS

Design dimensions	Values (µm)
Overall width of ground and substrate	650.75
Overall length of ground and substrate	379.54
Length of the feed to the first patch	23.53
Length of the feed to the second patch	126.47
Lower width of the patch from the feed	28.49
Distance between two dual patches	320
Feeding height from the substrate	119.75
Distance between the center of the dual patches to the center feed	170
Distance between the center of the dual patches to the substrate	108.41
Height of the feeding to the patch	88.64

Table II presents the design dimensions of the 1×4 array antenna, which were used in the simulation environment to model the proposed structure. The return loss (S_{11}) parameter as a function of frequency is plotted in Figure 12. A pronounced dip is observed at 0.8 THz, where the return loss falls below −25 dB (with a minimum of −28 dB), indicating an effective impedance matching and minimal reflection.

Figure 13 illustrates the antenna gain across the frequency range, showing a stable radiation performance with a peak gain of approximately 11 dBi at 0.85 THz. These results confirm the suitability of the proposed design for high-frequency wireless applications.

A comparative analysis between the proposed antenna and previously reported designs is presented below, highlighting the differences in gain, bandwidth, and return loss (S_{11}). Table III summarizes these comparisons. Among the referenced designs, the one in [5] exhibits the lowest return loss (−67.2 dB), followed closely by that in [12] at −64.16 dB, with all demonstrating excellent impedance matching characteristics.

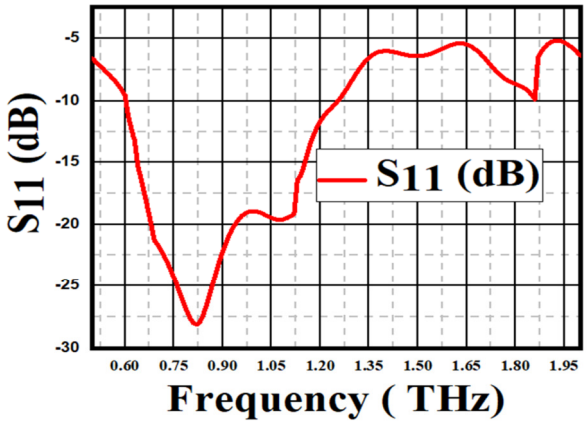

Fig. 12. Return loss (S_{11}) of the 1×4 linear array antenna.

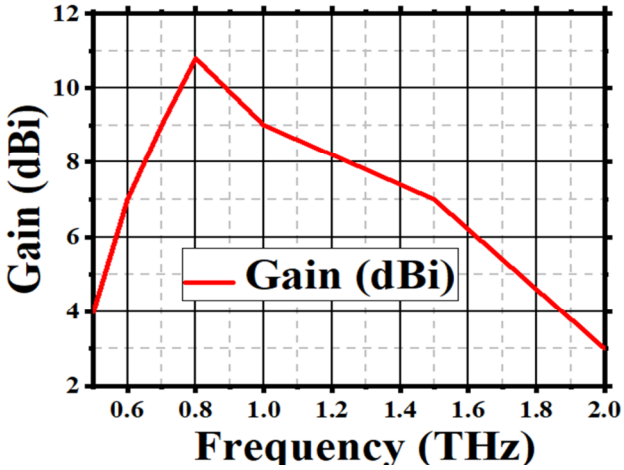

Fig. 13. Simulated gain of the 1×4 linear array antenna.

III. COMPARISON OF RESULTS

TABLE III. COMPARISON WITH PREVIOUS STUDIES

Reference	S11 (dB)	Bandwidth (THz)	Gain (dBi)
[1]	-27.08	1.25	7.769
[4]	-64.16	0.0267	6.793
[5]	−64.16	0.024	6.793
[6]	-57.54	0.1996	2.76
[7]	-28	0.038	5
[8]	-24.5	0.415	5.587
[9]	-16.86	0.092	6.14
[13]	−26.27	0.02	6.32
[14]	−67.2	0.03	9.75
[15]	−14.5	0.036	4.92
[16]	-34	0.022	1.8
This work	-28	1	11

These designs, however, have very limited bandwidths, with 0.03 THz, 0.0267 THz, and 0.024 THz. The advantage of these designs is the use of a photonic bandgap and defected ground structure to get better impedance matching. On the other hand, the design of [1] boasts the largest bandwidth at 1.25 THz, with a reasonable gain of 7.769dBi and return loss of −27.08dB. The disadvantage of this design is the low gain because many slots are etched on the patch. By attaining a bandwidth of 0.415 THz, a gain of 5.587dBi, and a return loss of −24.5 dB, other studies, like [8], provide a mild trade-off. The advantage of this design is the use of graphene-based patch antennas, but the disadvantage is the low gain due to two different types of patch antennas. The proposed design performs well overall, with a high bandwidth of 1.0 THz, second only to that of [1], and a return loss of −28 dB, indicating good impedance matching. Among all the designs that were compared, it obtains the maximum gain of 11dBi, surpassing even that of [5], which had a gain of 9.75dBi. This work shows a better trade-off between the bandwidth, gain, and return loss than previous research. A solid option for applications needing high efficiency, wideband, and directional THz radiation, this approach maintains great performance across all three parameters, unlike some studies that excel in only one, such as [3, 5] in return loss or [1] in bandwidth. In addition, the advantage of the designs in [16, 17] is the Polymer Dispersed Liquid Crystal (PDLC) and Substrate Integrated Waveguide (SIW) technique to obtain a better return loss.

IV. CONCLUSIONS AND FUTURE SCOPE OF WORK

A four-step design methodology is employed to develop the proposed antenna for Terahertz (THz)-band Sixth Generation (6G) wireless communication applications. In the first step, a basic rectangular microstrip patch antenna is designed, and its performance is evaluated in terms of the gain and return loss (S_{11}). The initial simulation yields a gain of 5.8 dBi and a return loss of −18 dB. In the second step, a triangular slot technique is applied to the rectangular patch to enhance performance. This modification improves the antenna's characteristics, achieving a gain of 7 dBi and a return loss of −21 dB.

Step 3 focuses on evaluating the mutual coupling coefficient between two identical patch antennas arranged in a linear configuration. A coupling coefficient of −18 dB is obtained, which is acceptable for wireless communication applications. In the final step, a 1×4 linear array antenna is designed and simulated to further enhance performance. Compared to Step 2, the array configuration achieves superior results, with a peak gain of 11 dBi and a return loss of −28 dB—the highest values observed throughout the design process.

Future work will explore different feeding techniques, alternative substrate materials, and the extension of the array to include more elements for a higher gain. In addition, broader 6G applications will require experimental validation, further structural optimization, and potential integration into more complex communication systems

REFERENCES

[1] R. H. Masum *et al.*, "A Slotted Elliptical Patch Antenna for Six Generation Communication System in Terahertz Band," *Cureus Journals*, vol. 2, no. 1, Jan. 2025, https://doi.org/10.7759/s44388-024-02717-3.

[2] K. C. Rao, P. M. Rao, M. L. Naidu, and V. Adiarayana, "A Compact Rectangular Dual Patch Antenna for Multiple Satellite Communication Applications," *Wireless Personal Communications*, vol. 122, no. 2, pp. 1007–1041, Jan. 2022, https://doi.org/10.1007/s11277-021-08937-8.

[3] R. Pant and L. Malviya, "THz antennas design, developments, challenges, and applications: A review," *International Journal of Communication Systems*, vol. 36, no. 8, 2023, Art. no. e5474, https://doi.org/10.1002/dac.5474.

[4] S. Mrunalini and A. Manoharan, "Dual-Band Reconfigurable Graphene based Patch antenna in Terahertz band for WNoC Applications," *IET Microwaves, Antennas & Propagation*, vol. 11, Aug. 2017, https://doi.org/10.1049/iet-map.2017.0415.

[5] S. Ullah, Ruan ,Cunjun, Haq ,Tanveer Ul, and X. and Zhang, "High performance THz patch antenna using photonic band gap and defected ground structure," *Journal of Electromagnetic Waves and Applications*, vol. 33, no. 15, pp. 1943–1954, Oct. 2019, https://doi.org/10.1080/09205071.2019.1654929.

[6] Md. A. K. Khan, T. A. Shaem, and M. A. Alim, "Analysis of graphene based miniaturized terahertz patch antennas for single band and dual band operation," *Optik*, vol. 194, Oct. 2019, Art. no. 163012, https://doi.org/10.1016/j.ijleo.2019.163012.

[7] K. Vijayalakshmi, C. S. K. Selvi, and B. Sapna, "Novel tri-band series fed microstrip antenna array for THz MIMO communications," *Optical and Quantum Electronics*, vol. 53, no. 7, Jul. 2021, Art. no. 395, https://doi.org/10.1007/s11082-021-03065-w.

[8] W. A. Khan and A. Bin Muhammad, "Design and Analysis of Wideband THz Micro Size Patch Antenna for 6G application," in *2022 6th International Conference on Millimeter-Wave and Terahertz Technologies (MMWaTT)*, Sep. 2022, pp. 1–4, https://doi.org/10.1109/MMWaTT58022.2022.10172086.

[9] K. K. Naik, "Asymmetric CPW-fed patch antenna with slits at terahertz applications for 6G wireless communications," *Wireless Networks*, vol. 30, no. 4, pp. 2343–2351, May 2024, https://doi.org/10.1007/s11276-024-03695-4.

[10] M. Gezimati and G. Singh, "Terahertz Imaging and Sensing for Healthcare: Current Status and Future Perspectives," *IEEE Access*, vol. 11, pp. 18590–18619, Feb. 2023, https://doi.org/10.1109/ACCESS.2023.3247196.

[11] X. Ji *et al.*, "Design of High-Gain Antenna Arrays for Terahertz Applications," *Micromachines*, vol. 15, no. 3, Mar. 2024, Art. no. 407, https://doi.org/10.3390/mi15030407.

[12] M. Khulbe, M. R. Tripathy, H. Parthasarthy, and J. Dhondhiyal, "Dual Band THz Antenna Using T Structures and Effect of Substrate Volume on Antenna Parameters," in *2016 8th International Conference on Computational Intelligence and Communication Networks (CICN)*, Sep. 2016, pp. 191–195, https://doi.org/10.1109/CICN.2016.43.

[13] A. Bendaoudi, M. Berka, M. Debab, and Z. Mahdjoub, "Effects of ground plane on a square graphene ribbon patch antenna designed on a high-permittivity substrate with PBG structures," *Frequenz*, vol. 77, no. 7–8, pp. 385–394, Aug. 2023, https://doi.org/10.1515/freq-2022-0149.

[14] M. N. eddine Temmar, A. Hocini, D. Khedrouche, and T. A. Denidni, "Enhanced Flexible Terahertz Microstrip Antenna Based on Modified Silicon-Air Photonic Crystal," *Optik*, vol. 217, Sep. 2020, Art. no. 164897, https://doi.org/10.1016/j.ijleo.2020.164897.

[15] P. Garu and W.-C. Wang, "Design and Analysis of a PDLC-Based Reconfigurable Hilbert Fractal Antenna for Large and Fine THz Frequency Tuning," *Micromachines*, vol. 13, no. 6, Jun. 2022, Art. no. 964, https://doi.org/10.3390/mi13060964.

[16] A. A. Althuwayb, "On-Chip Antenna Design Using the Concepts of Metamaterial and SIW Principles Applicable to Terahertz Integrated Circuits Operating over 0.6–0.622 THz," *International Journal of Antennas and Propagation*, vol. 2020, no. 1, Dec. 2020, Art. no. 6653095, https://doi.org/10.1155/2020/6653095.